Article

Not peer-reviewed version

Obtaining of Nitride on the Surface of Single-Crystalline Germanium for Photocatalytic Research

Irakli Nakhutsrishvil * , Sandro Bakhtadze , Sema Guseinova

Posted Date: 25 November 2025

doi: 10.20944/preprints202511.1935.v1

Keywords: germanium; hydrazine; nitride; catalysis

 doi:10.20944/preprints202511.1935.v1

Article

Obtaining of Nitride on the Surface of Single-Crystalline Germanium for Photocatalytic Research

Irakli Nakhutsrishvili [1,*], Sandro Bakhtadze [2] and Sema Guseinova [3]

[1] Georgian Technical University, 77 Kostava St., 0171 Tbilisi
[2] Geoaeronavigation Company, Airport St., 0158 Tbilisi
[3] Tbilisi State University, 1 Chavchavadze av., 0128 Tbilisi
* Correspondence: iraklinakhutsrishvili52@gmail.com

Abstract

The paper presented here examines the decomposition of hydrazine on the surface of single-crystalline germanium at 650°C, the kinetics of the nitride formation process at ≥650°C was studied using a microgravimetric method and the question of the possibility of using α-Ge_3N_4 and mixtures of α- and β-Ge_3N_4 as a photocatalyst was considered.

Keywords: germanium; hydrazine; nitride; catalysis

1. Introduction

Germanium nitride Ge_3N_4 finds application in micro- and nanoelectronics, photoluminescence, energy storage, photocatalysis [1–10] and others. Usually Ge_3N_4 is obtained by interaction of ammonia with elemental germanium at (650-700) °C or its dioxide (GeO_2) at (700-750) °C:

$3Ge+4NH_3 \longrightarrow Ge_3N_4+6H_2$, (1)

$3GeO_2+4NH_3 \longrightarrow Ge_3N_4+6H_2O$. (2)

According to reaction (1), the α-modification of nitride is formed, and according to reaction (2), the β-modification (*).

An original method is also the use of hydrazine vapors [16]:

$3Ge+2N_2H_4 \longrightarrow Ge_3N_4+4H_2$. (3)

(*) Germanium nitride exists in the form of several crystal modifications: α-, β-, γ-, δ- Ge_3N_4 [11–13]. The t-, m-, o-modifications of nitride are also theoretically discussed [14,15] (α, β, δ – hexagonal, γ – cubic, t – tetragonal, m – monoclinic, o – orthorhombic syngony). At normal temperatures and pressures, only the α- and β-modifications are stable.

Bot modifications consist of $Ge(N_4)$ tetrahedra and crystallize in hexagonal syngonia. The difference between them lies in the arrangement of $Ge(N_4)$ tetrahedra along the "c" axis (Figure 1). The values of elementary cell parameters from various literature data are given in Table 1. Figure 2 shows their elementary cells.

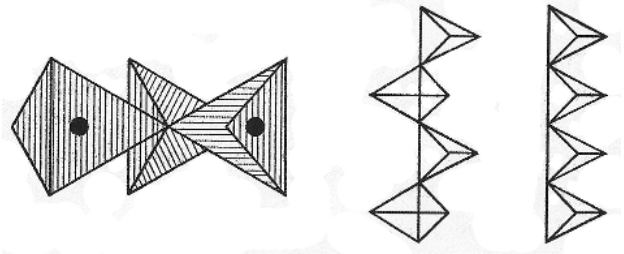

α-Ge_3N_4 β-Ge_3N_4

(a) (b)

 doi:10.20944/preprints202511.1935.v1

Figure 1. (a) - Triplets of $Ge(N_4)$ tetrahedra (in the center - Ge, on the peaks - N) and (b) - arrangement of tetrahedra along the "c" axis (vertical direction).

Table 1. – Parameters of elementary cells of α- and β-Ge_3N_4.

modif. / par.,Å	α-Ge_3N_4	β- Ge_3N_4
a	8.202[11],7.985[12]	8.038[11], 7.826[12], 8.119[13]
c	5.94[11], 5.786[12]	3.074[11],3.993[12], 3.104[13]

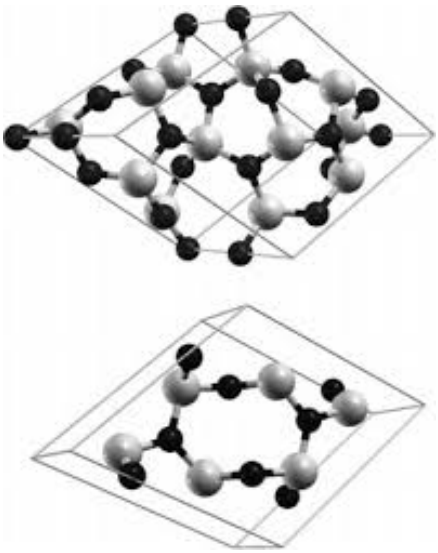

Figure 2. Elementary cells of germanium nitride: (a) α-Ge_3N_4, (b) β-Ge_3N_4.

Below it will be shown that at 650°C hydrazine in the presence of germanium decomposes according to the scheme:

$2N_2H_4 \rightarrow 2NH_3+N_2+H_2$. (4)

It is known that at experimentally achievable temperatures and pressures, nitrogen does not interact with germanium, and the Ge-H bond is broken below 650°C. Therefore, in hydrazine vapors, nitride is actually formed according to scheme (1). Since germanium is an active catalyst for the decomposition reaction of hydrazine, this issue will be discussed in detail.

2. Materials & Reagents

Commertial hydrazine-hydrate containing 50 mol.% (36 wt.%) water was distilled using the Raschig's method with improvement. In particular, before distillation, it was boiled with NaOH in an inert atmosphere of nitrogen at a temperature of 120°C for two hours. Hydrazine purified in this way had a density of $\varrho \cong 1.0024$ g/cm^3 and a refractive index of $n_D^{20} \cong 1.4705$. According to the literature, this latter value corresponds to 100% N_2H_4. However, this can be considered not entirely correct.

Plates of single-crystalline germanium doped with antimony (charge carrier concentration $n \cong 2 \cdot 10^{14}$cm^{-3}) had a resistivity of ≅35 Ohm·cm. The crystallographic orientation of Ge plates are (111) or (100). They were previously degreased in boiling toluene, etched in liquid etchant $HF:HNO_3:CH_3COOH$=1:15:1 for 4-5 minutes and washed in running distilled water.

 doi:10.20944/preprints202511.1935.v1

3. Results and Discussion

3.1. Decomposition of Hydrazine on the Surface of Single-Crystalline Germanium

Hydrazine is one of the most chemically active substances - a strong reducing agent. He has wide application in various fields of industry, technology, medicine, etc. and has been intensively studied both previously and currently [14–25]. Liquid N_2H_4 is very hygroscopicand has a noticeable ability to absorb oxygen and carbon dioxide from the air. It is called "high purity" when the water content does not exceed 1 wt.% and "ultra-pure" - with a maximum of 0.5 wt.% H_2O. The concentration of water in hydrazine is estimated by the density, melting point, or refractive index of the mixture. However, literature data on these parameters are different, due to the difficulty of accurately determining the physical characteristics of pure hydrazine (*).

Hydrazine is easily decomposed by heat and radiation, especially in the presence of catalysts [35–38]. The general form of this reaction is given by the equation:

$3N_2H_4 \rightarrow 4(1-x)\ NH_3+(1+2x)\ N_2+6xH_2$. (5)

(*) According to various authors, the density of liquid hydrazine at 25°C is 1.0045, 1.0036 and 1.0024, 1.008 g/cm^3 at 23°C. The melting point of the system N_2H_4/H_2O: 1, 1.4, 1.53, 1.6-1.7, 1.8, 1.85 and 2°C [26–28].

Depending on external conditions (temperature, pressure, catalyst, electromagnetic radiation, electric discharge, etc.) $0 \leq x \leq 1$(*). The catalytic decomposition of hydrazine on the surface of germanium has been studied relatively littleand there is data when carrying out the reaction up to 80°C. In early work [32], powders of Ge of n- and p-type conductivity were used. It was found that the decomposition products were ammonia and nitrogen:

$3N_2H_4 \rightarrow NH_3+N_2$.(6)

The type of conductivity did not affect the catalytic properties.

Figure 3a shows the kinetic curves of the accumulation of hydrogen and ammonia at 650°C. It can be seen that the amount of ammonia is constant in the absence of germanium, and in its presence gradually decreases. The hydrogen content in the presence of Ge increases sharply, and in its absence it first increases and then decreases. The resulting ammonia corresponds to an equimolar amount of chemisorbed hydrazine. As a result, the total change of pressure (Figure 3b) is determined only by the decomposition reaction.

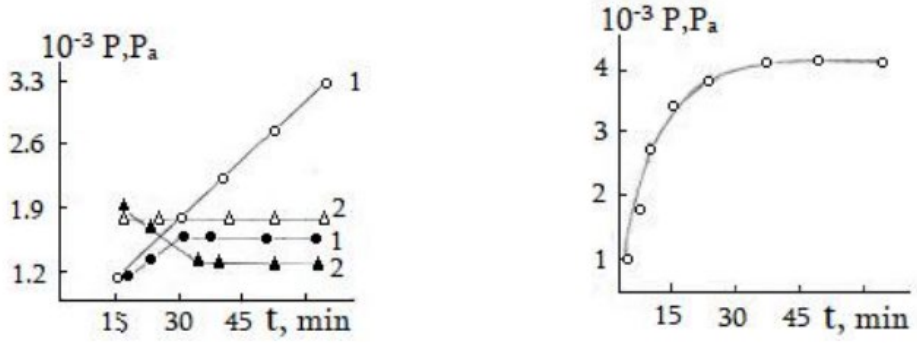

(a) (b)

Figure 3. (a) Kinetic curves of hydrogen (1) and ammonia (2) accumulation during the decomposition of hydrazine in the presence of germanium (●, ▲) and without it (o, Δ); (b) kinetic curve of the total change of pressure of gaseous products at 650°C.

Thermodynamic calculation of the change of free energy showed that reaction (5) at x = 0.25 (i.e. reaction (4)) has almost the same probability as reaction (6): change in Gibbs free energy $\Delta G \cong 220.5$ and $\cong 222.6$ kJ/mol respectively (**). However, the discovered fact of hydrogen evolution gives preference to reaction (4).

 doi:10.20944/preprints202511.1935.v1

(*) On alkaline catalysts x=1, on some semiconductor catalysts (Ga, Ga_2Se_3 and others), as well as on some metals (Te, Pt) x=0, on some semiconductors (V_2O_5, Ga_2Te_3 and others), as well as on acid catalysts 0<x<1, during decomposition using a spark x = 0.38, and during bombardment with α-particles x = 0.12-0.22 [29–31].

(**) The estimate of ΔG should be considered approximate since a change in pressure occurs in the reaction area.

A sharp increase of the amount of hydrogen and a decrease of the amount of ammonia in the presence of germanium can be associated with a heterogeneous reaction (1).

The study of high-temperature decomposition of hydrazine was also carried out using IR absorption spectra. Figure 4 shows the IR spectra of N_2H_4 vapor, demonstrating the dynamics of its decomposition at 650°C. Curve 1 corresponds to hydrazine vapor, curves 2 and 3 to hydrazine heated for 15 and 30 minutes, and curve 4 to pure ammonia. These spectra indicate that the decomposition of hydrazine at 650°C occurs mainly during the first 15 minutes and is completely completed within 30 minutes.

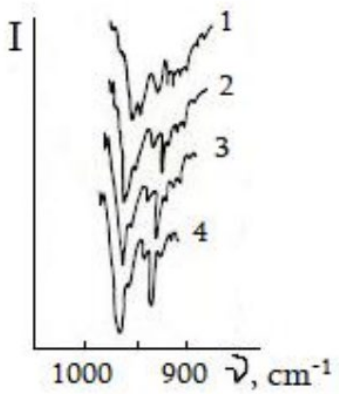

Figure 4. Dynamics of hydrazine decomposition at 650°C in presence of germanium.

3.2. Formation of Nitride on Germanium Surface

At temperatures >650°C, nitride Ge_3N_4 is formed in hydrazine vapor on the surface of germanium, and by registration mass change of the sample using the microgravimetric method, the following processes are observed[16]: first, an increase of mass occurs due to the accumulation of hydrazine and its decomposition products on the surface, then the mass of the sample decreases due to etching of Ge with contained in hydrazine water vapors, and then observes its gradual increase due to formation of Ge_3N_4.

 doi:10.20944/preprints202511.1935.v1

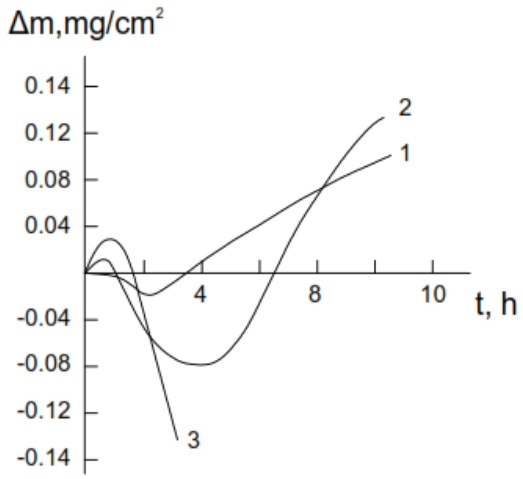

Figure 5. The kinetic curves of the interaction of hydrazine vapors with germanium at 700°C: 1 - the process carried out immediately after distillation, 2 - after two weeks, 3 - after a month.

It should be noted that when freshly distilled hydrazine was stored in a special ampoule under vacuum, over fairly long periods of time (two weeks, a month), we did not detect any change in determining of the refractive index within the measurement accuracy. However, a significant difference in the nitridation kinetics was observed (Figure 5). From this figure, in particular, one can see the difference in the etching rates of the germanium surface at the same temperature[33]. This can be attributed to the gradual humidization of hydrazine, despite precautions. Really, under the above conditions, the following occurs: first, β-Ge_3N_4 is formed, and then traces of α-modification are observed in the nitride. When hydrazine is specially hydrated, the amount of α-Ge_3N_4 increases and it is finally possible to obtain it in pure form[34].

It should also be noted that the initial increase of mass (Figure 5) is 2-3 orders of magnitude greater than is typical for physical adsorption. This can be associated with the accumulation of polar molecules of hydrazine and water with high dipole moments (~2 D[35,36]) on the germanium surface.

One can also take into account the existence of hydrazine in the imide tautomeric form:

$H_2N\text{-}NH_2 \leftrightarrow N^-H\text{-}N^+H_3$.

The bipolar imide form of hydrazine is characterized by a pronounced ability to associate molecules and a strong donor property to atoms with unfilled d- and f-shells, especially in substances with a small band gap (for example, germanium).

The above can be confirmed by the results of supplementary experiments on the interaction of germanium with ammonia, as with a molecule of the amine form. At the initial stage of this reaction at (500-700) °C, we observed an increase in the sample by (2-4) μg/cm², which is characteristic of the process of physical adsorption of neutral molecules.

3.3. The Possibility of Using of Germanium Nitride as a Photocatalyst in the Conversion of Carbon Monoxide to Dioxide

The role of photocatalysis in natural photosynthesis, energy, biotechnology, ecology, other fields of science and technology, or in solving household problems is widely known. Among the compounds that are studied to achieve the catalytic effect by visible or ultraviolet radiation, non-oxide materials occupy an important place. Among them are simple (binary) nitrides: C_3N_4 [37–41], GaN [42–44], TiN [45,46], Ta_3N_5 [47,48], HfN [49,50], Si_3N_4 [51,52], Ge_3N_4.

The essence of photocatalysis is to increase of the rate or excitation of chemical reactions under the influence of light in the presence of substances that absorb light quanta and participate in the chemical transformations of these substances, repeatedly entering into intermediate interactions with them and regenerating their chemical composition after each cycle. (A simplified diagram of the

 doi:10.20944/preprints202511.1935.v1

process is shown in Figure 6.) All this became possible after the fundamental works of A. Fujishima [53–57].

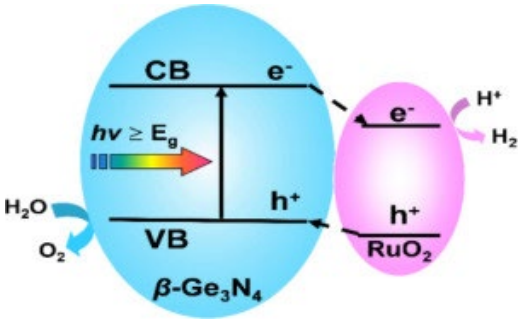

Figure 6. – Schematic representation of the photocatalytic process of water splitting[10].

As noted in the introduction, germanium nitride was successfully tested using photoradiation in the process of water splitting. The authors of the cited works used β-Ge_3N_4 doped with RuO_2.

The authors of this paper are currently conducting experiments to determine the photocatalytic activity of Ge_3N_4 for converting CO into CO_2. We use α-Ge_3N_4 and mixtures of α- and β-modifications doped with platinum or palladium. It is evident from the Figure 2 that this modification of the nitride is capable of dissolving the dopant in itself more effectively (*).

4. Conclusions

At ≥650°C hydrazine decomposes on the surface of single-crystalline germanium according to the scheme: $2N_2H_4 \rightarrow 2NH_3+N_2+H_2$. A sharp increase in the amount of hydrogen and a decrease in the amount of ammonia in the presence of germanium is observed. This is due to a heterogeneous reaction: $3Ge+4NH_3 \rightarrow Ge_3N_4+6H_2$. The phase composition of solid product of this reaction is an indicator of the degree of humidity of hydrazine: in pure hydrazine vapors, β-Ge_3N_4 is formed on the surface of germanium, and as water is added, a mixture of α- and β-modifications is formed until pure α-Ge_3N_4 is formed. The question of the possibility of using α-Ge_3N_4 and mixtures of α- and β-Ge_3N_4 as a photocatalyst was considered.

(*) The problem of converting toxic CO into harmless CO_2 is a very urgent task[58-66]. Purification of atmospheric air from harmful substances is of great importance for human health. One of the main sources of air pollution are internal combustion engines, namely cars. The most toxic component of their exhaust gases is precisely carbon monoxide. CO is especially dangerous because, due to its physical properties, it enters people's homes or workplaces more easily than other toxic exhaust gas components. It is odorless and cannot be detected by the senses. The most effective means of protecting residential and workplaces of people from carbon dioxide are cleaning devices containing photocatalysts, which, under the conditions of the use of an appropriate catalyst and natural air convection, will effectively purify them from CO.

References

1. Mallem K, Jagadeesh Chandra S V, Ju M et al., Influence of ultra-thin Ge_3N_4 passivation layer on structural, interfacial, and electrical properties of HfO_2/Ge Metal-Oxide–Semiconductor devices. *Nanosci Nanotechn*, 20 (2020), 1039.
2. Okamoto G, Kutsuki K, Hosoi T. et al., 2011. Electrical characteristics of Ge-based metal-insulator-semiconductor devices with Ge3N4 dielectrics formed by plasma nitridation. *Nanosci and Nanotechn*, 11 (2011), 2856.
3. 3Huang Z, Su R, Yuan H et al., Synthesis and photoluminescence of ultra-pure α-Ge_3N_4 nanowires. *Ceramics Intern*, 4, (2018), 10858.

 doi:10.20944/preprints202511.1935.v1

4. Kim Sh, Hwang G, Jung J-W et al., Fast, scalable synthesis of micronized Ge_3N_4 @C with a high tap density for excellent lithium storage. *Adv Funct Mater*, 7 (2017), 1605975.
5. Maggoini G, Carturan S, Fiorese L et al., Germanium nitride and oxynitride films for surface passivation of Ge radiation detectors. *Appl Surface Sci*, 393 (2017), 119.
6. Yayak Y O, Sozen Y, Tan F et al., First-principles investigation of structural, Raman and electronic characteristics of single layer Ge_3N_4. *Appl Surface Sci*, 572 (2022), 15136.
7. Sato J, Saito N, Yasmada Y et al., RuO_2-loaded β-Ge_3N_4 as a non-oxide photocatalyst for overall water splitting. *Amer Chem Soc*, 127 (2005), 4150.
8. Lee Y, Watanabe T, Takata T et al., Effect of high-pressure ammonia treatment on the activity of Ge_3N_4 photocatalyst for overall water splitting. *Phys Chem B*, 110 (2006), 17563.
9. 9Maeda K & Domen K, New non-oxide photocatalysts designed for overall water splitting under visible light. *Phys Chem C*, 111, (2007), 7851.
10. Ma Y, Wang M & Zhou X, First-principles investigation of β-Ge_3N_4 loaded with RuO_2 cocatalysts for photocatalytic overall water splitting. *Energy Chem*, 44 (2020), 24-32.
11. Ruddlesden S & Popper D, On the crystal structures of the nitrides of silicon and germanium. *Acta Cryst*, 11 (1958), 465-469.
12. Sevic C & Bulutay C, Theoretical study of the insulating oxides and nitrides. *Mater Sci*, 42 (2007), 6555.
13. Luo Y, Cang Y & Chen D, 2014. Determination of the finite temperature anisotropic elastic and thermal properties of Ge_3N_4: A first principle study. *Computat Condens Matt*, 1 (2014), 1, 1.
14. Cang Y, Chen D, Yang F & Yang H, 2016. Theoretical studies of tetragonal, monoclinic and orthorhombic distortions of germanium nitride polymorphs. *Chem Chinese Univ*, 37 (2016), 674.
15. Cang Y, Yao X, Chen D et al., First-principles study on the electronic, elastic and thermodynamic properties of tree novel germanium nitrides. *Semiconduct*, 37 (2016), 072002.
16. Nakhutsrishvili I, Study of growth and sublimation of germanium nitride using the concept of Tedmon's kinetic model. Oriental J Chem, 36 (2020), 850.
17. Audrieth L F & Mohr P H, 1948. The chemistry of hydrazine. *Chem Eng News*, 26 (1948), 3746.
18. Audrieth L F & Ogg B A, The chemistry of hydrazines. John Wiley & Sons: New York, USA, (1951), 256.
19. Schmidt E W, One hundred years of hydrazine chemistry. Proceedings of 3rd Conference on Environmental Chemistry of Hydrazine Fuels: 15-17 September 1987, Florida, USA, 4-16.
20. 20Krishnadasan A, Kennedy N, Zhao Y & Morgenstern H, Nested case-control study of occupational chemical exposures and prostate cancer in aerospace and radiation workers. *Amer Industrial Medic*, 50, (2007), 383.
21. 21Turner J L, Rocket and spacecraft propulsion: Principles, practice and new developments. Springer Praxis Books. Prax. Publ. LTD: New York, USA, 2009, 390.
22. 22 Schmidt E W & Gordon M S, The decomposition of hydrazine in the gas phase and over an iridium catalyst. Zeitsch. Phys. Chem., 227, (2013), 1301.
23. 23 Chen Y, Zhao Ch, Liu X et al., 2023. Multi-scene visual hydrazine hydrate detection based on a dibenzothiazole derivative. *Analyst*, 148 (2022), 856.
24. 24 Yan K, Yan L, Kuang W et al., Novel biosynthesis of gold nanoparticles for multifunctional applications: Electrochemical detection of hydrazine and treatment of gastric cancer. *Environm Res*, 238, (2023), 117081.
25. *Zhang G, Zhu Z*, Chen Y et al., Direct hydrazine borane fuel cells using non-noble carbon-supported polypyrrole cobalt hydroxide as an anode catalyst. *Sustain Energy Fuels*, *7*, (2023), *2594.*

 doi:10.20944/preprints202511.1935.v1

26. Luo F, Pan Ch, Xie Y et al., Hydrazine-assisted acidic water splitting driven by iridium single atoms. *Adv Sci*, 10, (2023), 2305058.
27. Burilov V A, Belov R N, *Solovieva S E &* Antipin I S, Hydrazine-assisted one-pot depropargylation and reduction of functionalized nitro calix[4]arenes. *Russ Chem Bull*, 72 (2023), 948.
28. Rennebaum T, van Gerven D, Sean S et al., Hydrazine sulfonic acid, $NH_3NH(SO_3)$, the bigger sibling of sulfamic acid. *Chem Europe*, 30, (2024), e202302526.
29. Elts E, Windmann T, Staak D & Vrabec J, Fluid phase behavior from molecular simulation: Hydrazine, Monomethylhydrazine, Dimethylhydrazine and binary mixtures containing these compounds. *Fluid Phase Equilibr*, 322/323 (2012), 79.
30. Ahlert R C, Bauerle G L & Lecce J V, Density and viscosity of anhydrous hydrazine at elevated temperatures. *Chem Eng Data*, 7, (1962), 158.
31. Zhao B, Song J, Ran R & Shao Z, Catalytic decomposition of hydrous hydrazine to hydrogen over oxide catalysts at ambient conditions for PEMFCs. *Hydrogen Energy*, 1 (2012), 1133.
32. Frolov V M., Catalytic decomposition of hydrazine on germanium. *Russ Kinetics and Catalysis,* 6 (1965), 149.
33. Nakhutsrishvili I, Adamia Z & Kakhniashvili G, Gas etching of germanium surface with water vapors contained in nitrogen-containing reagents. *Appl Surface Sci*, 2, (2024), 1.
34. Vardosanidze Z, Nakhutsrishvili I & Kokhreidze R, Conditions of formation of α- and β-modifications of Ge_3N_4 and preparation of germanium oxynitride dielectric films. *Coating Sci and Techn*, 11 (2024), 1.
35. Ekong A, Akpan V A & Ebomwonyi O, DMC and VMC calculations of the electric dipole moment and the ground-state total energy of hydrazine molecule using CASINO-code. *Lett Chem Phys and Astronomy*, 59 (2015), 106.
36. Krylov O V, Frolov V M, Fokina E A & Rufov Yu N, Catalytic decomposition of hydrazine. 8th Mendeleev Congress on General and Applied Chemistry - Section of Physical Chemistry: 16-23 March 1958, Moskow, USSR, 172.
37. Ye J, Wan Y & Li Y, Construction of dual S-scheme heterojunctions g-C_3N_4/CoAl LDH@MIL-53(Fe) ternary photocatalyst for enhanced photocatalytic H_2 evolution. Appl. Surface Sci., 2025, 684, 161862.
38. Wtulich M, Skwierawska A, Ibragimov S & Lisowska–Oleksial A, Exploring the role of carbon nitrides (melem, melon, g-C_3N_4) in enhancing photoelectrocatalytic properties of TiO_2 nanotubes for water electrooxidation. *Appl Surface Sci*, 685 (2025), 161994.
39. Mohapatra L, Paramanik L, Choi D & Yoo S H, Advancing photocatalytic performance for enhanced visible-light-driven H_2 evolution and Cr(VI) reduction of g-C_3N_4 through defect engineering via electron beam irradiation. *Appl Surface Sci*, 685 (2025), 161996.
40. Sharma P, Mukherjee D, Sakar S et al., Pd doped carbon nitride (Pd-g-C_3N_4): an efficient photocatalyst for hydrogenation *via* an Al–H_2O system and an electrocatalyst towards overall water splitting. *Green Chem*, 24 (2022), 5535.
41. Chen J, Fang S, Shen Q et al., Recent advances of doping and surface modifying carbon nitride with characterization techniques. *Catalysts*, 12 (2022), 962.
42. Ohkawa K, Ohara W, Ushida D & Deura M, Highly stable GaN photocatalyst for producing H_2 gas from water. *Japan Appl Phys*, 52 (2013), 08JH04.
43. Shimosako N & Sakama H, Quantum efficiency of photocatalytic activity by GaN films. *AIP Adv*, 11 (2021), 025019.
44. Schäfer S. Wyrzgol A, Caterino R et al., Platinum nanoparticles on gallium nitride surfaces: Effect of semiconductor doping on nanoparticle reactivity. *Amer Chem Soc*, 134 (2012), 12528.

 doi:10.20944/preprints202511.1935.v1

45. Guler U, Suslov S, Kildishev A V et al., Colloidal plasmonic titanium nitride nanoparticles: properties and applications. *Nanophotonics*, 4 (2015), 269.
46. Zhou X, Zolnhofer E M, Nguyen N T et al., Stable cocatalyst-free photocatalytic H_2 evolution from oxidized titanium nitride nanopowders. *Angew Chem*, 54, (2015), 13385.
47. Ma S S K, Hisatomi T, Maeda K et al., Enhanced water oxidation on Ta_3N_5 photocatalysts by modification with alkaline metal alts. *Amer Chem Soc*, 134 (2012), 19993.
48. Harb M & Basset J-M, Predicting the most suitable surface candidates of Ta_3N_5 photocatalysts for water-splitting reactions using screened coulomb hybrid DFT computations. *Phys Chem C*, 124 (2020), 2472.
49. Shirvani F & Shokri A, Photocatalytic applicability of HfN and tuning it with Mg and Sc alloys: A DFT and molecular dynamic survey. *Phys B: Condensed Matter*, 649 (2023), 414459.
50. O'neill D B, Frehan S K, Zhu K et al., Ultrafast photoinduced heat generation by plasmonic HfN nanoparticles. *Adv Opt Materials*, 9 (2021), 2100510.
51. Yang Q, Chen Z, Yang X et al., Facile synthesis of Si_3N_4 nanowires with enhanced photocatalytic applications. *Materials Lett*, 212 (2018), 41.
52. Munif A N, Firas J & Kadhim F J, Structural characteristics and photocatalytic activity of TiO_2/Si_3N_4 nanocomposite synthesized via plasma sputtering technique. *Iraqi Phys*, 22 (2024), 99.
53. Fujishima A, Rao T N & Tryk D A, Titanium dioxide photocatalysis. *Photochem and Photobiol C: Photochem Rev*, 1 (2000), 1.
54. Seifikar F & Habibi-Yangjeh A, Floating photocatalysts as promising materials for environmental detoxification and energy production: A review. *Chemosphere*, 355 (2024), 141686.
55. Mohamadpour F & Amani A M, Photocatalytic systems: reactions, mechanism, and applications. *RSC Adv*, 14 (2024), 20609.
56. Beil S B, Bonnet S, Casadevall C et al., Challenges and future perspectives in photocatalysis: Conclusions from an interdisciplinary workshop. *JACS*, 4 (2024), 2746.
57. Chakravorty A & Roy S, A review of photocatalysis, basic principles, processes, and materials. *Sust Chem Envir*, 8 (2024), 100155.
58. Haag W M, Methods to reduce carbon monoxide levels at the workplace. *Preventive Medic*, 8 (1979), 369.
59. Samadi P, Binczarski M J, Pawlaczyk A et al., CO oxidation over Pd catalyst supported on porous TiO_2 prepared by plasma electrolytic oxidation (PEO) of a Ti metallic carrier. *Materials*, 15 (2022), 4301.
60. Kersell H, Hooshmand Z, G. Yan G et al., CO oxidation mechanisms on CoO_x-Pt thin films. *Amer Chem Soc*, 142 (2020), 8312.
61. Rostami A A, Hajaligol M, Li P et al., Formation and reduction of carbon monoxide. *Beiträge zur Tabakforsch Intern*, 20 (2014), 439.
62. Antony A G, Radhakrishnan K, Saravanan K & Vijayan V, 2020. Reduction of carbon monoxide content from four stroke petrol engine by using subsystem. *Vehicle Struct. & Systems*, 12 (2020), 384.
63. Mamilov S, Yesman S, Mantareva V et al., Optical method for reduction of carbon monoxide intoxication. *Bulg Chem Commun*, 52 (2020), 142.
64. Bujak J, Sitarz P & Pasela R, 2021. Possibilities for reducing CO and TOC emissions in thermal waste treatment plants: A case study. *Energies*, 14 (2021), 2901.
65. Ruqia B, Tomboc G M, Kwon T et al., Recent advances in the electrochemical CO reduction reaction towards highly selective formation of Cx products (X = 1–3). *Chem Catalysis*, 2 (2022), 1961.
66. Wilbur Sh, Williams M, Williams R et al., Toxicological profile for carbon monoxide. Agency for Toxic Substances and Disease Registry: Atlanta, USA. Bookshelf ID: NBK153696 (2012).

 doi:10.20944/preprints202511.1935.v1